

Cathodic Detection of H₂O₂ Using Iodide-Modified Gold Electrode in Alkaline Media

Md. Rezwan Miah[†] and Takeo Ohsaka*

Department of Electronic Chemistry, Interdisciplinary Graduate School of Science and Engineering,
Tokyo Institute of Technology, Mail Box G1-5, 4259 Nagatsuta, Midori-ku, Yokohama 226-8502, Japan

Oxidative chemisorption and cathodic stripping reductive desorption of iodide have been studied at a smooth polycrystalline gold (Au (poly)) electrode. Potential-dependent surface coverage of iodide has been controlled on the basis of its reductive desorption in 0.1 M KOH alkaline media and its quantitative oxidation to aqueous iodates in acidic media. The Au (poly) electrode surface catalyzes the decomposition of H₂O₂ to O₂. Specific adsorption of iodide on the Au electrode inhibits fully the catalytic decomposition and electrochemical oxidation of H₂O₂ as well as the adsorption of unknown impurities and the oxidative degradation of the electrode surface by H₂O₂. A quantitative characterization/detection of H₂O₂ at the iodide-modified Au (poly) electrode in the alkaline media has, thus, been achieved. Performance of the electrode toward the detection of H₂O₂ with respect to response time and sensitivity as well as operational stability has been evaluated. It has a sensitivity of 0.272 mA cm⁻² mM⁻¹ in amperometric measurements with a detection limit of 1.0 × 10⁻⁵ M H₂O₂, and the response time to achieve 95% of the steady-state current is <20 s. The effect of O₂ in the air-saturated solution can be minimized by subtracting the additional current for the O₂ reduction. Experimental measurements were based upon cyclic voltametric and amperometric techniques.

The electrochemical reduction of hydrogen peroxide (H₂O₂) at Pt, Au, and Ag electrodes (bare and modified) and various metal alloys is of great interest in connection with development of fuel cells because H₂O₂ is an important intermediate of the oxygen reduction reaction (basic electrochemical reaction in fuel cells). It is also important in terms of developing biosensors for determining H₂O₂ in food, pharmaceutical, clinical, industrial, and environmental analyses.^{1–19} Numerous electrochemical sensors

based on the use of different chemicals, such as myoglobin,¹ (3-mercaptopropyl)trimethoxysilane,² Prussian Blue,^{3–5} cyclopentadienylnickel(II)thiolato Schiffbase,⁶ tris(2,2'-bipyridil)copper(II) chloride complex,⁷ hemoglobin,⁸ manganese hexacyanoferrate,⁹ horseradish peroxidase (with and without mediators),^{10–17,20–27} etc., have been used for the determination of H₂O₂. Many of the sensors so far developed show a satisfactory sensitivity for the detection of relatively lower concentrations of H₂O₂. But detection of relatively higher concentrations of H₂O₂, especially at metal electrodes and carbon electrodes modified by metal particles, is still challenging because of the rapid decomposition of H₂O₂ catalyzed by metal electrodes themselves and the lowering of the electrode surface activity.²⁷ Moreover, these sensors have problems with respect to price, stability, reproducibility, and portability. In this paper, we propose a new approach to the electrochemical detection of relatively higher concentrations of H₂O₂ in alkaline media by using a I⁻-modified gold electrode based on the potential-dependent desorption/adsorption behavior of I⁻ on a gold electrode as well as the unique potential dependence of I⁻ adlayer structures. I⁻ adlayers fully block the electrode surface and thus inhibit the surface catalytic decomposition of H₂O₂. At relatively lower potentials, I⁻ adlayers undergo the reductive desorption, and the reduction of H₂O₂ reproducibly takes place at the in situ-created highly fresh electrode surface.

* To whom correspondence should be addressed. Phone: +81-45-9245404. Fax: +81-45-9245489. E-mail: ohsaka@chem.titech.ac.jp.

[†] Permanent address: Department of Chemistry, School of Physical Sciences, Shahjalal University of Science and Technology, Sylhet-3114, Bangladesh.

(1) Dai, Z.; Xu, X.; Ju, H. *Anal. Biochem.* **2004**, *332*, 23.

(2) Shankaran, D. R.; Iimura, K. I.; Kato, T. *Sens. Actuators, B* **2003**, *96*, 523.

(3) De Mattos, I. L.; Gorton, L.; Ruzgas, T. *Biosens. Bioelectron.* **2003**, *18*, 193.

(4) Garjonyte, R.; Malinauskas, A. *Sens. Actuators, B* **1999**, *56*, 93.

(5) Florito, P. A.; de Torresi, S. I. C. *Talanta* **2004**, *62*, 649.

(6) Morrin, A.; Moutloali, R. M.; Killard, A. J.; Smyth, M. R.; Darkwa, J.; Iwuoha, E. I. *Talanta* **2004**, *64*, 30.

(7) Sotomayor, M. D. P. T.; Tanaka, A. A.; Kubota, L. T. *Electrochim. Acta* **2003**, *48*, 855.

(8) Gu, H.-Y.; Yu, A.-M.; Chen, H.-Y. *J. Electroanal. Chem.* **2001**, *516*, 119.

(9) Eftekhari, A. *Talanta* **2001**, *55*, 395.

(10) Lei, C.-X.; Hu, S.-Q.; Shen, G.-L.; Yu, R.-Q. *Talanta* **2003**, *59*, 981.

(11) Tatsuma, T.; Ogawa, T.; Sato, R.; Oyama, N. *J. Electroanal. Chem.* **2001**, *501*, 180.

(12) Dong, S.; Li, J. *Bioelectrochem. Bioenerg.* **1997**, *42*, 7.

(13) Kong, Y.-T.; Boopathi, M.; Shim, Y.-B. *Biosens. Bioelectron.* **2003**, *42*, 227.

(14) Mao, L.; Yamamoto, K. *Talanta* **2000**, *51*, 187.

(15) Sun, D.; Cai, C.; Li, X.; Xing, W.; Lu, T. *J. Electroanal. Chem.* **2004**, *566*, 415.

(16) Ferapontova, E.; Paganova, E. *J. Electroanal. Chem.* **2002**, *518*, 20.

(17) Ferapontova, E.; Gorton, L. *Bioelectrochem.* **2002**, *55*, 83.

(18) Daly, D. J.; O'Sullivan, C. K.; Guilbault, G. G. *Talanta* **1999**, *49*, 667.

(19) Shimizu, Y.; Komatsu, H.; Michishita, S.; Miura, N.; Yamazo, N. *Sens. Actuators, B* **1996**, *34*, 493.

(20) Karyakin, A. A.; Karyakina, E. E.; Gorton, L. *Anal. Chem.* **2000**, *72*, 1720.

(21) Karyakin, A. A.; Paganova, E. A.; Budashov, I. A.; Kurochkin, I. N.; Karyakina, E. E.; Levchenko, V. A.; Matveyenko, V. N.; Varfolomeyev, S. D. *Anal. Chem.* **2004**, *76*, 474.

(22) Karyakin, A. A.; Gitelmacher, O. V.; Karyakina, E. E. *Anal. Chem.* **1995**, *67*, 2419.

(23) Kenausis, G.; Chen, Q.; Heller, A. *Anal. Chem.* **1997**, *69*, 1054.

(24) Gorton, L. *Electroanalysis* **1995**, *7*, 23.

(25) Wang, J.; Liu, J.; Chen, L.; Lu, F. *Anal. Chem.* **1994**, *66*, 3600.

(26) O'Connell, P. J.; O'Sullivan, C. K.; Guilbault, G. G. *Anal. Chim. Acta* **1988**, *373*, 261.

(27) Gerlache, M.; Grousi, S.; Quarin, G.; Kauffmann, J.-M. *Electrochim. Acta* **1998**, *43*, 3461.

The structure of halide (X^-), especially iodide (I^-) adlayers at different metallic electrodes^{28–43} has recently become a subject of extensive studies because of its practical applications, such as (i) formation of highly ordered arrays of organic molecules,^{44,45} (ii) protection of highly sensitive surfaces of metal single crystals,^{46,47} (iii) underpotential deposition (UPD) of metallic adlayers of a desired structure,^{48,49} (iv) synthesis of nanoparticles rich in expected facets,⁵⁰ and (v) a test of catalytic activity by active site blocking strategy,⁵¹ etc. Furthermore, structures of ordered I^- overlayers have been investigated by many ex situ and in situ techniques, such as low-energy electron diffraction (LEED), Auger electron spectroscopy (AES) and X-ray photoelectron spectroscopy (XPS),^{28,29} surface enhanced Raman scattering (SERS),³⁰ scanning tunneling microscopy (STM),^{31–38} atomic force microscopy (AFM),³⁹ surface X-ray scattering (SXS),^{40,41} and electrochemical quartz crystal microbalance (ECQM),^{42,43} etc. The remarkable point derived from these studies is that I^- adlayer structures are potential-dependent. For example, at a more positive potential, a closely packed hexagonal structure exists, and it blocks the access of solution species to the electrode surface. In other words, as the electrode potential becomes more negative, the desorption of I^- occurs, which results in a free space for species to reach the electrode surface and to give their electrochemical response. Adzic et al. have studied the effect of the structures of bromide (Br^-) adlayers at different single crystalline electrodes on the oxygen reduction reaction (ORR).^{52,53} Effects of different halide adlayers at the polycrystalline Ag electrode on ORR have been explored by Brandt.⁵⁴ Surface concentration, Gibbs energies of adsorption, and electrosorption valance for I^- at the Au (111) electrode have been determined by Lipkowski et al.⁵⁵

Here, we report the effects of I^- adlayers at a Au (poly) electrode on H_2O_2 reduction reaction in alkaline media. Sensing of H_2O_2 using this I^- -modified electrode has been performed by

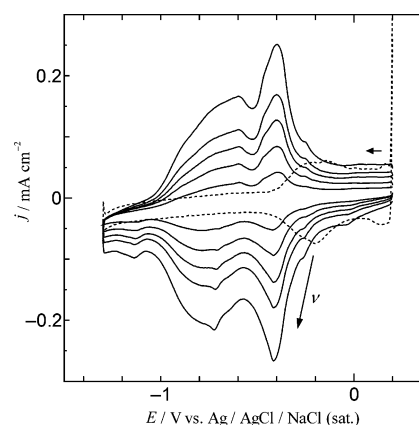


Figure 1. CVs obtained at the Au (poly) electrode in N_2 -saturated 0.1 M KOH solution containing 0.0 (dotted line) and 12.5 (solid lines) mM KI. Potential scan rates: 0.1 (dotted line) and 0.05, 0.1, 0.15, 0.2, 0.3 (solid lines) $V s^{-1}$.

cyclic voltametric and amperometric techniques, and its sensor characteristics have been examined in terms of potential-dependent adlayer structures of I^- and its inhibitory effect on catalytic decomposition of H_2O_2 .

EXPERIMENTAL SECTION

For cyclic voltametric measurements, Au (poly) electrodes ($\phi = 1.6$ mm sealed in a Teflon jacket) with an exposed surface area of $2.01 \times 10^{-2} \text{ cm}^2$ were used as working electrodes. A spiral Pt wire and a $Ag|AgCl|NaCl$ (sat.) were the counter and reference electrodes, respectively. A conventional two-compartment Pyrex glass cell was used. Prior to measurements, N_2 gas was bubbled into the cell for 30 min to obtain a N_2 -saturated KOH solution. The necessary amount of H_2O_2 was added into the solution. All the measurements were performed at $25 \pm 1^\circ C$. The Au (poly) electrodes were polished with aqueous slurries of successively finer alumina powder (down to $0.06 \mu m$), sonicated for 10 min in Milli-Q water, and then electrochemically pretreated in 0.05 M H_2SO_4 solution by repeating the potential scan in the range of -0.2 to 1.5 V vs $Ag|AgCl|NaCl$ (sat.) at $0.1 V s^{-1}$ for 10 min or until the cyclic voltametric characteristic for a clean Au electrode was obtained. A roughness factor (rf) of 1.2 was estimated for the Au (poly) electrodes as calculated from the charge consumed during the formation of the surface oxide monolayer.⁵⁶ Chemisorption of I^- at the electrode was ensured by adding 12.5 mM KI in to an aqueous solution of 0.1 M KOH. Experiments were always performed in the presence of added KI if otherwise not mentioned. Oxidation of chemisorbed I^- was performed in N_2 -saturated 0.05 M H_2SO_4 solution to determine potential-dependent surface coverage of I^- ($\theta_{I,E}$). The Au (poly) electrode with I^- adlayer is hereafter denoted as $I^-|Au$ (poly) electrode. Electrochemical measurements were performed using an ALS CHI-832A electrochemical analyzer.

RESULTS AND DISCUSSION

Chemisorption of I^- at the Au (poly) Electrode. Figure 1 shows the cyclic voltammograms (CVs) obtained at the Au (poly) electrode in N_2 -saturated 0.1 M KOH solution containing 0.0

- (28) Batina, N.; Yamada, T.; Itaya, K. *Langmuir* **1995**, *11*, 4568.
- (29) Bravo, B. G.; Michelhaugh, S. L.; Soriaga, M. P.; Villegas, I.; Suggs, D. W.; Stickney, J. L. *J. Phys. Chem.* **1991**, *95*, 5245.
- (30) Gao, P.; Weaver, M. J. *J. Phys. Chem.* **1986**, *90*, 4057.
- (31) Gao, X.; Weaver, M. J. *J. Am. Chem. Soc.* **1992**, *114*, 8544.
- (32) Matsumoto, H.; Inukai, J.; Ito, M. *J. Electroanal. Chem.* **1994**, *379*, 223.
- (33) Tao, N. J.; Lindsay, S. M. *J. Phys. Chem.* **1992**, *96*, 5213.
- (34) Gao, X.; Edens, G. J.; Weaver, M. J. *J. Phys. Chem.* **1994**, *98*, 8074.
- (35) Haiss, W.; Sass, J. K.; Gao, X.; Weaver, M. J. *Surf. Sci.* **1992**, *274*, L593.
- (36) McCarty, R. L.; Bard, A. J. *J. Phys. Chem.* **1991**, *95*, 9618.
- (37) Yamada, T.; Batina, N.; Itaya, K. *Surf. Sci.* **1995**, *335*, 204.
- (38) Yamada, T.; Batina, N.; Itaya, K. *J. Phys. Chem.* **1995**, *99*, 8817.
- (39) Hasse, U.; Scholz, F. *Electrochem. Commun.* **2004**, *6*, 409.
- (40) Wu, X. Z.; Ocko, B. M.; Sirota, E. B.; Sinha, S. K.; Deutsch, M. *Physica A* **1993**, *200*, 751.
- (41) Ocko, B. M.; Watson, G. M.; Wang, J. J. *J. Phys. Chem.* **1994**, *98*, 897.
- (42) Lei, H.-W.; Uchida, H.; Watanabe, M. *J. Electroanal. Chem.* **1996**, *413*, 131.
- (43) Lei, H.-W.; Uchida, H.; Watanabe, M. *Langmuir* **1997**, *13*, 3523.
- (44) Kunitake, M.; Batina, N.; Itaya, K. *Langmuir* **1995**, *11*, 2337.
- (45) Batina, N.; Kunitake, M.; Itaya, K. *J. Electroanal. Chem.* **1996**, *405*, 245.
- (46) Hubbard, A. T. *Chem. Rev.* **1998**, *88*, 633.
- (47) Soriaga, M. P. *Prog. Surf. Sci.* **1992**, *39*, 325.
- (48) Sugita, S.; Abe, T.; Itaya, K. *J. Phys. Chem.* **1993**, *39*, 8780.
- (49) Stickney, J. L.; Rosaco, S. D.; Hubbard, A. T. *J. Electrochem. Soc.* **1984**, *131*, 260.
- (50) Hernández, J.; Solla-Gullón, J.; Herrero, E. *J. Electroanal. Chem.* **2004**, *574*, 185.
- (51) Hsieh, S. J.; Gewirth, A. A. *Surf. Sci.* **2002**, *498*, 147.
- (52) Wang, J. X.; Marinkovic, N. S.; Adzic, R. R. *Colloids Surf.* **1998**, *134*, 165.
- (53) Adzic, R. R.; Wang, J. X. *Electrochim. Acta* **2000**, *45*, 4203.
- (54) Brandt, E. S. *J. Electroanal. Chem.* **1983**, *150*, 97.
- (55) Chen, A.; Shi, Z.; Bizzotto, D.; Lipkowski, J.; Pettinger, B.; Bilger, C. *J. Electroanal. Chem.* **1999**, *467*, 342.
- (56) Finot, M. O.; Braybrook, G. D.; McDermott, M. T. *J. Electroanal. Chem.* **1999**, *466*, 234.

(dotted line) and 12.5 (solid lines) mM KI at scan rates of 0.1 (dotted line) and 0.05, 0.1, 0.15, 0.2, 0.3 (solid lines) V s⁻¹. The couple of the anodic and cathodic peaks obtained at around -0.2 V in the absence of I⁻ corresponds to the partial oxidation (anodic scan) and reductive desorption (cathodic scan) of the chemisorbed hydroxyl ion, OH⁻.⁵⁷ In the presence of I⁻, the couple was diminished due to the blocking of the Au (poly) electrode surface by preferential chemisorption of I⁻.⁵³ The CV profile obtained in the presence of I⁻ is similar to that obtained by Stickney et al.²⁹ Sharp, symmetrical waves at -0.4 and -0.72 V are assigned to the adsorption/desorption of I⁻ at the Au (poly) electrode surface.²⁹ According to the value of θ_{LE} ,^{29,58} the whole potential zone under investigation can be divided into three groups: (i) $E > -0.2$ V, $\theta_{LE} \geq 0.4$ with a $(5 \times \sqrt{3})$ -I adlayer structure, (ii) -0.2 V $> E > -0.5$ V, $0.33 > \theta_{LE} > 0.25$ with a $(\sqrt{3} \times \sqrt{3})R30^\circ$ -I structure, and (iii) $E < -0.5$ V, $\theta_{LE} < 0.25$ with a (4×4) -I structure. At a potential above -0.2 V, the I⁻ row along the x axis is compressed as the electrode potential becomes more positive, resulting in a continuous increase of θ_{LE} from 0.33 to 0.4 and giving a rotated-hexagonal adlayer structure, $(5 \times \sqrt{3})$ -I.³⁸ This type of potential-dependent uniaxial compression of the I⁻ adlayer is termed electrocompression.^{37,59,60} At a potential below -0.2 V, continuous desorption of I⁻ occurs, leading to the conversion of a closely packed, rotated-hexagonal structure to a relatively less packed rectangular adlayer structure, $(\sqrt{3} \times \sqrt{3})R30^\circ$ -I.⁵³ The sharp cathodic peak at -0.4 V is attributed to such a kind of phase transition and decreasing of θ_{LE} from 0.33 to a lower value. As the potential becomes more negative than -0.4 V, θ_{LE} decreases continuously, resulting in some defects at the ordered $(\sqrt{3} \times \sqrt{3})$ - $R30^\circ$ -I structure and giving some holes. At a potential below -0.5 V, a broad cathodic peak is obtained due to more desorption ($\theta_{LE} < 0.25$) of I⁻ from the surface and a change of the $(\sqrt{3} \times \sqrt{3})R30^\circ$ -I to a (4×4) -I structure, resulting in an increase in the I-I distance. As the potential is swept to the positive direction, specific adsorption of I⁻ begins at a potential of -1.0 V^{29,58} and increases gradually up to -0.55 V. At a potential of -0.4 V, the rapid adsorption leads to an ordered $(\sqrt{3} \times \sqrt{3})$ - $R30^\circ$ -I structure. As the potential is swept to a more positive potential, more adsorption of I⁻ gives a rotated-hexagonal structure.

Figure 2 shows the LSVs obtained in N₂-saturated 0.05 M H₂SO₄ solution containing 0.0 (2–5) and 12.5 (1) mM KI at the Au (poly) (1, 5) and I⁻|Au (poly) (2–4) electrodes at a scan rate of 0.1 V s⁻¹. I⁻|Au (poly) electrodes were prepared by soaking the Au (poly) electrode in 12.5 mM KI-containing N₂-saturated 0.1 M KOH solution for 10 min and then sweeping the potential at a scan rate of 0.1 V s⁻¹ from an initial potential of 0.2 V to final potentials of (2) 0.0, (3) -0.49, and (4) -0.82 V for partial desorption of chemisorbed I⁻. LSV 5 (clean Au (poly)) contains three oxidation peaks at 1.08, 1.18, and 1.28 V. The presence of an I⁻ adlayer greatly modifies the LSV characteristics, that is, (i) the positive shift (more than 0.2 V) of the anodic peak observed

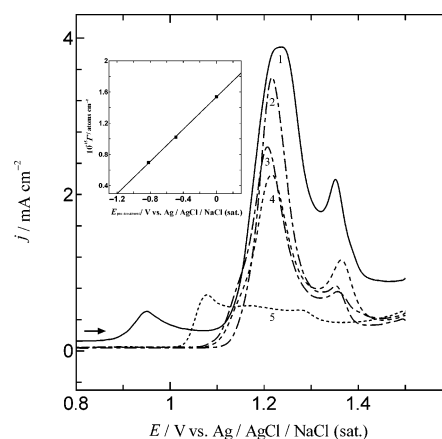
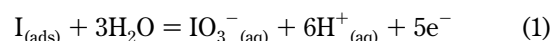


Figure 2. LSVs obtained at the Au (poly) (1, 5) and I⁻|Au (poly) (2–4) electrodes in N₂-saturated 0.05 M H₂SO₄ solution containing 0.0 (2–5) and 12.5 (1) mM KI. I⁻|Au (poly) electrode was treated by single linear sweep voltametric run in N₂-saturated 0.1 M KOH solution from an initial potential of 0.2 V to final potentials ($E_{\text{pretreatment}}$): (2) 0.0, (3) -0.49, and (4) -0.82 V. Potential scan rate: 0.1 V s⁻¹. Inset shows the plot of surface coverage of I⁻ (Γ_I) as a function of $E_{\text{pretreatment}}$.

at 1.08 V at the bare Au (poly) electrode and (ii) the remarkable increase in the oxidation peak intensities as compared to those obtained for the bare Au (poly) electrode.⁶¹ Similar phenomena have also been found for other noble metal electrodes, such as Pt, Ir, Rh, Ru, and Pd.⁶² The two well-defined anodic peaks at ~1.20 and 1.36 V are attributed to the oxidation of the specifically adsorbed I⁻ to oxoanions of iodine, such as iodates, together with the oxidation of the surface of the Au (poly) electrode itself.^{61,63} The iodate formation is expressed by eq 1.⁶³



With continuous potential cycling, the peak intensity decreases rapidly (in the cases of 2–4) to the Au (poly) electrode surface oxidation current. The characteristics of the LSVs from 1 to 4 are comparable, except for the gradual decrease of the peak intensity. LSV 2, which was recorded after sweeping the potential of the I⁻|Au (poly) electrode from 0.2 V to a final potential of 0.0 V may correspond to the oxidation of a monolayer of I⁻ at the Au (poly) electrode because θ_{LE} does not change so much at more positive potential than 0.0 V. A gradual decrease of the peak intensity in the cases of LSVs 3 and 4 reflects the gradual decrease of the amount of specifically adsorbed I⁻ by sweeping the potential of the I⁻|Au (poly) electrode from 0.2 V to -0.49 and -0.82 V; that is, the pretreatment potential becomes more negative. This observation also sustains the potential-dependent θ_{LE} values at the Au (poly) electrode.^{29,58} I⁻ undergoes quantitative oxidation to iodates in acidic media.⁶² The amount of the charge consumed for the oxidation of the specifically adsorbed I⁻ can be extracted by subtracting the Au (poly) electrode surface oxidation charge from the total oxidation charge (I⁻ + Au (poly) electrode), and

(57) Matsumoto, F.; Uesugi, S.; Koura, N.; Ohsaka, T. *J. Electroanal. Chem.* **2003**, 549, 71.

(58) Ocko, B. M.; Magnussen, O. M.; Wang, X. J.; Adzic, R. R.; Wandlowski, T. *Physica B* **1996**, 221, 238.

(59) Cuesta, A.; Kolb, D. M. *Surf. Sci.* **2000**, 465, 310.

(60) Broekmann, P.; Spaenig, A.; Hommes, A.; Wandelt, K. *Surf. Sci.* **2002**, 517, 123.

(61) Chang, C. C.; Yau, S. L.; Tu, J. W.; Yang, J. S. *Surf. Sci.* **2003**, 523, 59.

(62) Wan, L. J.; Yau, S. L.; Swain, G. M.; Itaya, K. *J. Electroanal. Chem.* **1995**, 381, 105.

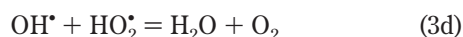
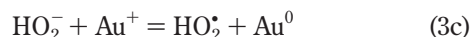
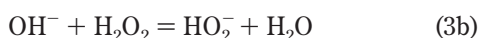
(63) Rodriguez, J. F.; Mebrahtu, T.; Soriaga, M. P. *J. Electroanal. Chem.* **1987**, 233, 283.

the surface coverage of I^- can be calculated by using eq 2,⁶³

$$\Gamma_{\text{I}} = Q/neA \quad (2)$$

where, Γ_{I} is the surface coverage of I^- , $n = 5$ according to eq 1, e is the charge of an electron (1.602177×10^{-19} C), and A is the geometric surface area of the Au (poly) electrode. The values of Γ_{I} at potentials 0.0, -0.49 , and -0.82 V were calculated as 1.54×10^{15} , 1.02×10^{15} , and 6.96×10^{14} atoms cm^{-2} , respectively, and are comparable to reported data.^{29,41} Γ_{I} was plotted as a function of the pretreatment potential ($E_{\text{pretreatment}}$) of the I^-/Au (poly) electrodes (inset in Figure 2). The values fall on a straight line similar to that found in the literature.^{29,58}

Behavior of H_2O_2 at the Bare Au (poly) Electrode. Inspection of Figure 3a, representing CV of 10 mM H_2O_2 in N_2 -saturated 0.1 M KOH solution within the potential window of 0.2 to -1.3 V recorded at the bare Au (poly) electrode at a scan rate of 0.1 V s^{-1} , reveals some remarkable features, that is, (i) a constant and nonzero oxidation current above the potential 0 V, (ii) a sharp cathodic peak at -0.165 V, (iii) a minor and relatively broad second cathodic peak at -0.895 V, and (iv) on the reverse scan, an ill-defined inverted peak having double waves at -0.306 and -0.165 V. The current plateau above 0 V is due to the electrochemical oxidation of H_2O_2 to O_2 . H_2O_2 in contact with the clean Au (poly) electrode undergoes a catalytic decomposition ($2\text{H}_2\text{O}_2 = 2\text{H}_2\text{O} + \text{O}_2$) according to eqs 3a–3d, shown below.^{64–67}



Numerous studies on the heterogeneous catalytic decomposition of H_2O_2 in contact with many metals are available.^{64–68} Decomposition of H_2O_2 is favored by a high solution pH⁶⁶ and a high positive potential.⁶⁴ Both electrochemical oxidation and catalytic decomposition of H_2O_2 supply O_2 that undergoes an electrochemical reduction, resulting in a cathodic peak at -0.165 V, even in the solution which contains no O_2 in its preparation step. CV c of Figure 3, recorded in O_2 -saturated H_2O_2 -free 0.1 M KOH solution, also shows a cathodic peak at the same potential for O_2 reduction. Therefore, the first cathodic peak is undoubtedly assigned to O_2 reduction, although the solution in which the voltammogram was recorded was initially N_2 -saturated. This cathodic peak strongly depends on the solution pH.⁶⁹ It disappears in acidic solutions because the catalytic decomposition of H_2O_2 at the Au (poly) electrode is inhibited. Its intensity gradually

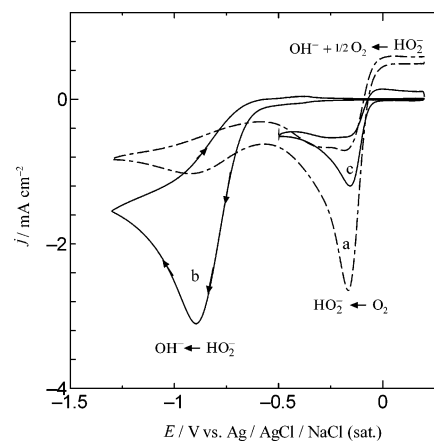


Figure 3. CVs obtained at the Au (poly) electrode in 10 (a, b) and 0.0 (c) mM H_2O_2 containing (a, b) N_2 - and (c) O_2 -saturated 0.1 M KOH solution without (a, c) and with (b) 12.5 mM KI. Potential scan rate: 0.1 V s^{-1} . Electrode was held in the solution for 10 min before measurements.

decreases as the upper potential limit becomes more negative as a result of a less feasible oxidation of H_2O_2 to O_2 .

The second cathodic peak at -0.895 V is assigned to the electrochemical reduction of H_2O_2 (exactly HO_2^- in this case) to OH^- .⁷⁰ Its poor intensity is due to the lower surface concentration of H_2O_2 because of its continuous decomposition and poor activity of the bare Au (poly) electrode for H_2O_2 oxidation. This peak current does not depend on the upper potential limit and is hardly reproducible, that is, quickly reduces on successive potential cycling. The inverted waves observed during the anodic sweep appear for O_2 (resulting from the decomposition of H_2O_2) reduction.⁶⁹ Therefore, the major obstacle to the quantitative characterization/detection of H_2O_2 in this media is its catalytic decomposition. Other notable problems are poor activity of the Au (poly) electrode, a lack of reproducibility, and uncertainty in determination of the second cathodic peak height because the (assumed) decaying current of the first wave must be used as the baseline.

Inhibition of H_2O_2 Decomposition at the I^-/Au (poly) Electrode. The catalytic decomposition of H_2O_2 is fully inhibited due to the formation of the closely packed hexagonal adlayer of I^- at the Au (poly) electrode where the I – I distance is narrow enough to prevent the permeation of H_2O_2 molecules to the electrode surface and, thus, to prevent reactions 3a–3d.⁵⁴ CV b of Figure 3 represents the reduction behavior of 10 mM H_2O_2 at the Au (poly) electrode in 12.5 mM KI containing N_2 -saturated 0.1 M KOH solution. Due to the closely packed adlayer of I^- , the electrochemical oxidation of H_2O_2 that appears above 0 V at the bare Au (poly) electrode has fully been inhibited. The oxygen reduction reaction that appears at ~ -0.5 V at the Au (poly) electrode in I^- -containing O_2 -saturated 0.1 M KOH solution has also disappeared because of the inhibition of both the electrochemical oxidation and the catalytic decomposition of H_2O_2 to O_2 . Unlike CV a of Figure 3, a well-defined reduction peak, assigned to the reduction of H_2O_2 , appears at -0.895 V, where a submonolayer ($\theta_{\text{LE}} < 0.25$) of I^- exists because of partial reductive desorption of the I^- monolayer.^{29,58} The peak potential is exactly the same as that of the second reduction peak obtained at the

(64) Merkulova, N. D.; Zhutaeva, G. V.; Shumilova, N. A.; Bagotzky, V. S. *Electrochim. Acta* **1973**, *18*, 169.

(65) Goszner, K.; Bischof, H. J. *Catal.* **1974**, *32*, 175.

(66) McKee, D. W. *J. Catal.* **1969**, *14*, 355.

(67) Bianchi, G.; Mazza, F.; Mussini, T. *Electrochim. Acta* **1962**, *7*, 457.

(68) Ishtchenko, V. V.; Huddersman, K. D.; Vitkovskaya, R. F. *Appl. Catal.* **2003**, *242*, 123.

(69) Prabhu, V. G.; Zarapkar, L. R.; Dhaneshwar, R. G. *Electrochim. Acta* **1981**, *26*, 725.

(70) Kongkanand, A.; Kuwabata, S. *Electrochem. Commun.* **2003**, *5*, 133.

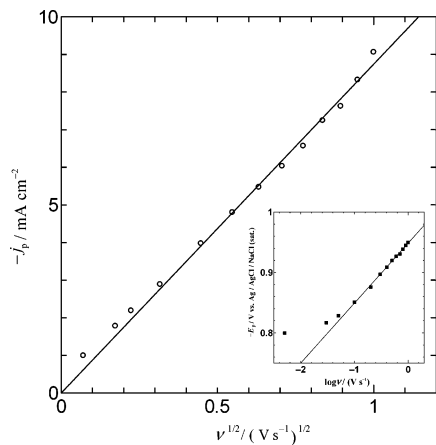


Figure 4. Linear plot of cathodic peak current intensity vs square root of scan rate. Inset shows the plot of peak potential vs $\log \nu$. Data were taken from CVs obtained at scan rates from 0.005 to 1.0 V s^{-1} .

bare Au (poly) electrode. The peak intensity obtained at the $\text{I}^-|\text{Au}$ (poly) electrode is comparable to that of the first cathodic peak for O_2 reduction, but it is ~ 7 times higher, as compared to the second peak obtained at the bare Au (poly) electrode, for the same concentration of H_2O_2 (compare CVs a and b). The cathodic peak at -0.895 V was highly reproducible due to the inhibition of the catalytic heterogeneous decomposition (expressed by eqs 3a–d) of H_2O_2 as well as the protection of the electrode surface from the adsorption of unknown impurities and the oxidative degradation by H_2O_2 , which is a strong oxidizing agent. The reduction of H_2O_2 in the present case takes place each time at the in situ-created highly fresh electrode surface, resulting in a satisfactory reproducibility in the detection of H_2O_2 . The reproducibility was also checked by recording CVs at scan rates ranging from 0.005 to 1.0 V s^{-1} . The cathodic peak current was plotted as a function of the square root of the scan rate (Figure 4). The best fitted straight line ($r^2 = 0.9972$) passes through the origin, and the points fall nicely on the straight line all over the scan rates, indicating that the H_2O_2 oxidation is diffusion-controlled.⁷¹ The peak potential has also been plotted as a function of $\log \nu$ and presented in the inset of Figure 4. Points in the potential zone of 0.1–1.0 V fall on a straight line ($r^2 = 0.9919$) having a slope of -0.099 V from which the cathodic transfer coefficient (α_c) was calculated to be 0.30.⁷²

Cyclic Voltammetric Detection. Figure 5 displays typical CVs obtained at the $\text{I}^-|\text{Au}$ (poly) electrode in 12.5 mM KI-containing N_2 -saturated 0.1 M KOH solution for H_2O_2 of concentrations (a) 0.1, (b) 2, (c) 4, (d) 6, (e) 8, and (f) 10 mM at a scan rate of 0.1 V s^{-1} . With increasing concentration, the peak current gradually increases. The cathodic peak currents of the CVs obtained for 0.01–150 mM of H_2O_2 were plotted as a function of the H_2O_2 concentration, as shown in Figure 6. A linear calibration curve was obtained for the H_2O_2 concentration ranging from 1.0×10^{-5} to 6.0×10^{-2} M (see inset), and at higher concentrations, the current deviated from linearity. The slope of the linear plot was $-0.243 \text{ mA cm}^{-2} \text{ mM}^{-1}$ with a correlation coefficient (r^2) of 0.9978 ($n = 10$). For comparison, the second reduction peak current obtained at the bare Au (poly) electrode in the same concentration range has also been plotted in Figure 6. The plot of j_p vs $[\text{H}_2\text{O}_2]$

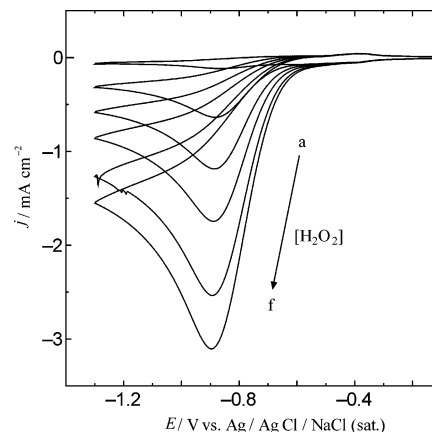


Figure 5. Typical CVs obtained at the Au (poly) electrode in N_2 -saturated 0.1 M KOH solution containing 12.5 mM KI and (a) 0.1, (b) 2, (c) 4, (d) 6, (e) 8, and (f) 10 mM H_2O_2 . Potential scan rate: 0.1 V s^{-1} .

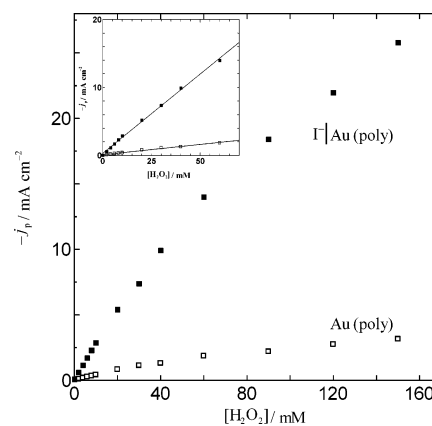


Figure 6. Typical plots of cathodic peak current intensity against H_2O_2 concentration ranging from 0.01 to 150 mM for the $\text{I}^-|\text{Au}$ (poly) and Au (poly) electrodes. Inset shows the linear plots in the range of 0.01–60 mM of H_2O_2 .

gave a slope of $-0.030 \text{ mA cm}^{-2} \text{ mM}^{-1}$ with a correlation coefficient of 0.9869 ($n = 10$). Thus, we can conclude that the $\text{I}^-|\text{Au}$ (poly) electrode possesses a much higher sensitivity for the cathodic detection of H_2O_2 , as compared with the unmodified Au (poly) electrode.

Amperometric Detection. We routinely performed chronoamperometric experiments at -1.1 V in N_2 -saturated 0.1 M KOH solution under a slow (100 rpm) solution-stirring condition.⁷³ The addition of H_2O_2 resulted in an apparent increase of the reduction current. The 95% response of the steady-state current was obtained within 20 s. This response time is comparable to those (20–30 s) of the tyrosine derivative and phenolic film-coated Pt^{73} and methylene green-immobilized, Nafion-coated, glassy carbon⁷⁴ electrodes, but longer than those (5–7 s) of the horseradish peroxidase⁷⁵ and myoglobin-immobilized⁷⁶ Au particle-modified ITO electrodes used for the detection of H_2O_2 in neutral phosphate buffer and acidic solutions, respectively. The response time was also similar to that of the bare Au (poly) electrode. The current response remained constant until a new sample was injected into the electrochemical cell.

(73) Long, D. D.; Marx, K. A.; Zhou, T. *J. Electroanal. Chem.* **2001**, 501, 107.

(74) Wang, B.; Dong, S. *Talanta* **2000**, 51, 565.

(75) Wang, L.; Wang, E. *Electrochem. Commun.* **2004**, 6, 225.

(76) Zhang, J.; Oyama, M. *J. Electroanal. Chem.* In press.

(71) Lu, W.; Wang, C.; Lv, Q.; Zhou, X. *J. Electroanal. Chem.* **2003**, 558, 59.

(72) Zhao, Y.-D.; Zang, W.-D.; Chen, H.; Luo, Q.-M. *Anal. Sci.* **2002**, 18, 939.

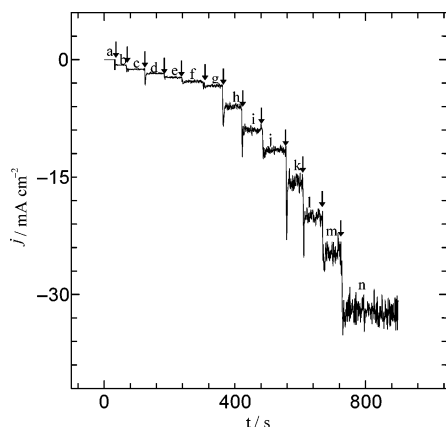


Figure 7. Typical current–time response obtained at the $\text{I}^-|\text{Au}$ (poly) electrode for various concentrations of H_2O_2 : (a) 0, (b) 2, (c) 4, (d) 6, (e) 8, (f) 10, (g) 12, (h) 20, (i) 30, (j) 40, (k) 60, (l) 90, (m) 120, and (n) 150 mM as a total concentration. The electrode was operated at -1.1 V in N_2 -saturated 0.1 M KOH solution containing 12.5 mM KI under stirring of the solution at 100 rpm. The arrows indicate the addition of H_2O_2 in the 0.1 M KOH solution.

Figure 7 illustrates a typical current–time response of the $\text{I}^-|\text{Au}$ (poly) electrode on successive step change of H_2O_2 concentration. The lowest detectable concentration is $\sim 1.0 \times 10^{-5}$ M, which is similar to the cyclic voltametric detection limit. Under the present condition, the steady-state current has a linear relationship with the concentration of H_2O_2 in the range from 1.0×10^{-5} to 6.0×10^{-2} M; that is, the linear plot gave a slope of -0.272 $\text{mA cm}^{-2} \text{mM}^{-1}$ with $r^2 = 0.9966$ ($n = 10$). Thus, the sensitivity of the modified electrode using cyclic voltametric and amperometric techniques is ~ 8 – 9 times higher, as compared to the bare Au (poly) electrode (0.0303 $\text{mA cm}^{-2} \text{mM}^{-1}$), and also higher than that of the electrodes previously used for the sensing of H_2O_2 at neutral pH.^{77–79}

Interference of Air, O_2 , Uric Acid, and Ascorbic Acid. O_2 in the air-saturated 0.1 M KOH solution undergoes the reduction at ~ -0.5 V at the $\text{I}^-|\text{Au}$ (poly) electrode to produce H_2O_2 , which can be further reduced at -0.895 V (see Figure 8). The current corresponding to the reduction of H_2O_2 resulting from the O_2 reduction can be determined from a blank experiment in the air-saturated 0.1 M KOH solution in the absence of H_2O_2 and can be subtracted from the total reduction current obtained in H_2O_2 -containing air-saturated solution. Thus, the effect of O_2 in air-saturated solution in determining the H_2O_2 concentration could be minimized. Addition of uric acid or ascorbic acid into the solution did not affect the cathodic peak current for the reduction of H_2O_2 .

Reproducibility, Repeatability, and Stability. Reproducibility of the current response of the electrode was investigated in air-saturated 0.1 M KOH solution containing 12.5 mM KI and 2 mM H_2O_2 by measuring the CVs five times every 30 min after holding the electrode in the solution. The relative standard deviation (RSD) was 1.1% ($n = 5$). For the interelectrode reproducibility of four electrodes in the same batch, the RSD was 3.5% . The stability of the electrode was investigated by storing the electrode with a full monolayer of I^- in air for 1–5 weeks and

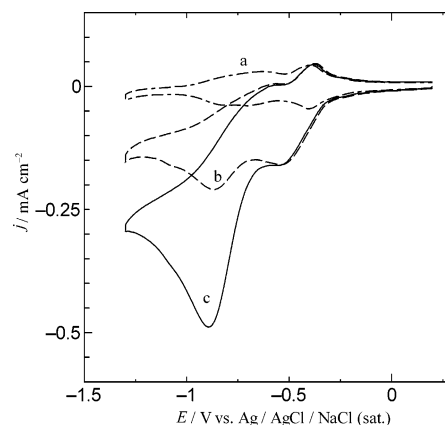


Figure 8. CVs obtained at the $\text{I}^-|\text{Au}$ (poly) electrode in (a) N_2 - and (b, c) air-saturated 0.1 M KOH solution containing 12.5 mM KI and (b) 0 and (c) 2.0 mM H_2O_2 . Potential scan rate: 0.1 V s^{-1} .

then measuring the current response of 2 mM H_2O_2 in air-saturated 0.1 M KOH solution containing 12.5 M KI. Current responses within a variation of 5% were achieved.

CONCLUSIONS

Reversible adsorption/desorption of I^- at the Au (poly) electrode in alkaline media has been studied with cyclic voltametry. Surface coverage of I^- increases with increasing potential, which is known as “electrocompression”.^{37,59,60} A full monolayer of I^- effectively inhibits the catalytic decomposition and electrochemical oxidation of H_2O_2 , which may occur usually at the bare Au (poly) electrode. The reduction of H_2O_2 takes place each time at the in situ-created, highly clean electrode surface. These enable us to detect H_2O_2 quantitatively using the $\text{I}^-|\text{Au}$ (poly) electrode. The calibration curves are linear over a wide range of H_2O_2 concentration, that is, 1.0×10^{-5} to 6.0×10^{-2} M. The sensitivity of the $\text{I}^-|\text{Au}$ (poly) electrode is ~ 8 – 9 times higher than that of the bare Au (poly) electrode. For the air-saturated sample solutions, the effect of O_2 can be minimized by subtracting the additional reduction current for H_2O_2 resulting from the O_2 reduction from the total reduction current. Addition of uric acid or ascorbic acid into the solution does not affect the cathodic peak current for the reduction of H_2O_2 . The electrode response is highly reproducible because of the inhibition of the surface catalytic decomposition of H_2O_2 as well as the protection of the electrode surface from the adsorption of unknown impurities and the oxidative degradation by H_2O_2 .

ACKNOWLEDGMENT

The present work was supported by the Grant-in-Aid for Scientific Research on Priority Areas (No. 417), Scientific Research (No. 12875164), and Scientific Research (A) (No. 10305064) to T. Ohsaka, from the Ministry of Education, Culture, Sports, Science and Technology of the Japanese Government (Monbu-Kagakusho) and also from the New Energy and Industrial Technology Development Organization (NEDO), Japan. Md. Rezwan Miah thanks the Government of Japan for the award of a scholarship by Monbu-Kagakusho.

Received for review September 6, 2005. Accepted December 7, 2005.

AC0515935

(77) Xu, Y.; Peng, W.; Liu, X.; Li, G. *Biosens. Bioelectron.* **2004**, *20*, 533.

(78) Li, J.; Tan, S. N.; Ge, H. *Anal. Chim. Acta* **1996**, *335*, 137.

(79) Wang, Q.; Lu, G.; Yang, B. *Sens. Actuators, B* **2004**, *99*, 50.